

Devil in the details: growth, productivity, and extinction risk of a data-sparse devil ray

Sebastián A. Pardo^{1*}, Holly K. Kindsvater^{1,2}, Elizabeth Cuevas-Zimbrón³, Oscar Sosa-Nishizaki⁴, Juan Carlos Pérez-Jiménez⁵, Nicholas K. Dulvy¹,

1 Earth to Ocean Research Group, Department of Biological Sciences, Simon Fraser University, Burnaby, BC, Canada

2 Department of Ecology, Evolution, and Natural Resources, Rutgers University, New Brunswick, NJ, USA

3 Fisheries Biology Consultant, Boulevard Chahue #66 Mz 6, Sector R, La Crucecita, Bahías de Huatulco, Oaxaca, Mexico

4 Laboratorio de Ecología Pesquera, Departamento de Oceanografía Biológica, CICESE, Ensenada, Baja California, Mexico

5 Ciencias de la Sustentabilidad, El Colegio de la Frontera Sur, Lerma, Campeche, Mexico

* Corresponding author: spardo@sfu.ca

1 Abstract

2 Devil rays (*Mobula* spp.) face rapidly intensifying fishing pressure to meet the ongoing interna-
3 tional trade and demand for their gill plates. This has been exacerbated by trade regulation of
4 manta ray gill plates following their 2014 CITES listing. Furthermore, the paucity of information
5 on growth, mortality, and fishing effort for devil rays make quantifying population growth rates
6 and extinction risk challenging. Here, we use a published size-at-age dataset for a large-bodied
7 devil ray species, the Spinetail Devil Ray (*Mobula japanica*), to estimate somatic growth rates,
8 age at maturity, maximum age and natural and fishing mortality. From these estimates, we go
9 on to calculate a plausible distribution of the maximum intrinsic population growth rate (r_{max})
10 and place the productivity of this large devil ray in context by comparing it to 95 other chon-
11 drichthyan species. We find evidence that larger devil rays have low somatic growth rate, low

12 annual reproductive output, and low maximum population growth rates, suggesting they have
13 low productivity. Devil ray maximum intrinsic population growth rate (r_{max}) is very similar to
14 that of manta rays, indicating devil rays can potentially be driven to local extinction at low levels
15 of fishing mortality. We show that fishing rates of a small-scale artisanal Mexican fishery were
16 up to three times greater than the natural mortality rate, and twice as high as our estimate of
17 r_{max} , and therefore unsustainable. Our approach can be applied to assess the limits of fishing
18 and extinction risk of any species with indeterminate growth, even with sparse size-at-age data.

19 Keywords: Bayesian, Euler-Lotka, catch-curve, Mobulidae, rebound potential, shark

20 **Introduction**

21 Understanding the sustainability and extinction risk of data-sparse species is a pressing problem
22 for policy-makers and managers. This challenge can be compounded by economic, social and
23 environmental actions, as in the case of the mobulid rays (subfamily Mobulinae). This group
24 includes two species of charismatic and relatively well-studied manta rays (*Manta* spp.), which
25 support a circumtropical dive tourism industry with an estimated worth of \$73 million USD per
26 year [1]. The Mobulinae also includes nine described species of devil rays (*Mobula* spp.). The re-
27 cent international trade regulation of manta ray gill plates under the Convention of International
28 Trade of Endangered Species (CITES) [2] is likely to shift gill plate demand from manta rays onto
29 devil rays.

30 Devil rays are increasingly threatened by target and incidental capture in a wide range of
31 fisheries, from small-scale artisanal to industrial trawl and purse seine fisheries targeting pelagic
32 fishes [3, 4]. The meat is sold on domestic markets and the gill plates are exported to meet con-
33 sumer demand, mostly from China [5]. Small-scale subsistence and artisanal fisheries, mainly for
34 meat, have operated throughout the world for decades [5]. For example, devil rays were caught
35 by artisanal fishermen using harpoons and gill nets around Bahia de La Ventana, Baja California,
36 Mexico, until 2007 when the Mexican government prohibited the take of mobulid rays [6].

37 Overall, around 90,000 devil rays are estimated to be caught annually in fisheries world-
38 wide [7]. Many industrial fleets capture devil rays incidentally. For example, European pelagic
39 trawlers in the Atlantic catch a range of megafauna including large devil rays at a rate of up to one
40 individual per hour [3], while purse seine fleets targeting tunas capture tens of thousands of devil
41 rays each year [4]. Even if devil rays are handled carefully and released, their post-release mortal-
42 ity might be significant [8]. We do not know whether the fisheries and international trade demand
43 for devil rays are significant enough to cause population declines and potential extinction. The
44 degree to which devil ray populations can withstand current patterns and levels of fishing mor-
45 tality depends on their intrinsic productivity, which determines their capacity to compensate for
46 fishing.

47 Slow somatic growth and large body size are associated with low productivity and elevated
48 threat status and extinction risk in marine fishes, including elasmobranchs [9–11]. Based on
49 these correlations, the American Fisheries Society developed criteria to define productivity and
50 extinction risk: They defined four levels of productivity (very low, low, medium, and high) based
51 on four life history traits (age at maturity, longevity, fecundity, and growth rate, which is related
52 to the von Bertalanffy growth coefficient k) and the intrinsic rate of population increase r [9].
53 According to these criteria, manta rays have very low or low productivity, with some of the lowest
54 maximum rates of population increase (r_{max}) of any shallow-water chondrichthyan [9, 12].

55 Here we evaluate the productivity, and hence relative extinction risk of large devils rays,
56 using the only age and growth study available for this group [13]. We use a Bayesian estimate of
57 somatic growth rate and a demographic model based on the Euler-Lotka equation to calculate the
58 maximum intrinsic rate of population increase (r_{max}) for a population of the Spinetail Devil Ray
59 *Mobula japanica* (Müller & Henle, 1841) and compare it to the productivity of 95 other sharks,
60 rays, and chimaeras.

61 **Methods**

62 We take advantage of the first study to measure length-at-age for catch data of *M. japonica* [13].
63 The Spinetail Devil Ray is similar in life history and size to other exploited mobulids, so we assume
64 it is representative of the relative risk of the group. Spinetail Devil Rays examined in this study
65 were caught seasonally by artisanal fishers using harpoon and gill nets around Punta Arenas de
66 la Ventana, Baja California Sur, Mexico, during the summers of 2002, 2004, and 2005 [13].

67 First, we estimate growth parameters using a Bayesian approach that incorporates prior knowl-
68 edge of maximum size and size at birth of this species, using the length-at-age data presented in
69 Cuevas-Zimbrón et al. (2013) [13] (Part 1). Second, we use the same dataset to plot a catch curve
70 of the relative frequency of individuals in each age-class, from which we can infer a total mor-
71 tality rate (Z) that includes both fishing (F) and natural mortality (M) (Part 2). This places an
72 upper bound on our estimate of natural mortality, and allows us to compare the observed rate
73 of mortality for this population with independent estimates of natural mortality rates. Third, we
74 estimate the maximum intrinsic rate of population increase (r_{max}) for this devil ray (Part 3) and
75 compare it against the r_{max} of 95 other chondrichthyans, calculated using the same method (Part
76 4).

77 **Part 1: Re-estimating von Bertalanffy growth parameters for the Spine-** 78 **tail Devil Ray.**

79 We analyse a unique set of length-at-age data for a single population of *M. japonica* caught in a
80 Mexican artisanal fishery. Individuals in this sample were limited to 110 and 240 cm disc width
81 (DW), which falls short (77%) of the maximum disc width reported elsewhere [14]. Therefore,
82 we use a Bayesian approach to refit growth curves to this length-at-age dataset [15]. We use
83 published estimates of maximum size and size at birth to set informative priors.

84 We fit the three-parameter von Bertalanffy equation to the length-at-age data, combining
85 sexes:

$$L_t = L_\infty - (L_\infty - L_0)e^{-kt} \quad (1)$$

86 where L_t is length at age t , and the growth coefficient k , size-at-age zero L_0 , and asymptotic
87 size L_∞ are the von Bertalanffy growth parameters. These parameters are conventionally pre-
88 sented in terms of length; here we use length synonymously with disc width, such that L_t , L_0 ,
89 L_∞ , and L_{max} are synonymous with DW_t , DW_0 , DW_∞ , and DW_{max} , respectively.

90 In order to account for multiplicative error, we log-transformed the von Bertalanffy growth
91 equation and added an error term:

$$\log(L_t) = \log(L_\infty - (L_\infty - L_0)e^{-kt}) + \epsilon_t \quad (2)$$

92 This can be written as:

$$\log(L_t) \sim Normal(\log(L_\infty - (L_\infty - L_0)e^{-kt}), \sigma^2) \quad (3)$$

93 A Bayesian approach allows us to incorporate expert knowledge using prior distributions
94 of estimated parameters. We based our informative priors on our knowledge of maximum disc
95 widths and size-at-birth of *M. japonica*. Reported size at birth ranges from 88 to 93 cm DW [16,17],
96 while reported maximum size for *M. japonica* is 310 cm DW [18]. While this reported maximum
97 size is from an individual recorded in New Zealand, we use this estimate as genetic evidence sug-
98 gests that populations of Spinetail Devil Rays in the Pacific Ocean have little genetic substruc-
99 ture [19]. Asymptotic size can be estimated from maximum size in fishes using the following
100 equation [20]:

$$L_\infty = 10^{0.044+0.9841*(\log(L_{max}))} \quad (4)$$

101 where L_{max} is maximum size, in centimetres. This results in an estimate of $L_\infty = 1.01 * L_{max}$
102 for a value of $L_{max} = 310$ cm DW. Instead of setting a fixed value for the conversion parameter, we

103 create a hyperprior for this parameter, defined as $kappa$, based on a gamma distribution around
104 a mean of 1.01. We concentrated the probability distribution of $kappa$ between 0.9 and 1.1, and
105 fully constrain it between 0.7 and 1.3 [20]:

$$kappa \sim Gamma(1000, 990) \quad (5)$$

106 We also constrain our prior for L_0 around size at birth, and use a beta distribution to constrain
107 our prior for growth coefficient k between zero and one, with a probability distribution that is
108 slightly higher closer to a value of 0.1:

$$k \sim Beta(1.05, 1.5)$$

$$L_\infty \sim Normal(3100 * kappa, 100) \quad (6)$$

$$L_0 \sim Normal(880, 200)$$

109 We compared the effect of our informative priors on our posteriors with parameter estimates
110 with weaker priors, in which we maintained the mean of the distributions but increased their
111 variance:

$$k \sim Beta(1.05, 1.1)$$

$$kappa \sim Gamma(200, 198) \quad (7)$$

$$L_\infty \sim Normal(3100 * kappa, 400)$$

$$L_0 \sim Normal(880, 300)$$

112 We also considered a scenario with uninformative priors, where all prior distributions are
113 uniform:

$$\begin{aligned}k &\sim \text{Uniform}(0, 2) \\kappa &\sim \text{Uniform}(0.7, 1.3) \\L_\infty &\sim \text{Uniform}(0, 4000) \\L_0 &\sim \text{Uniform}(0, 2000)\end{aligned}\tag{8}$$

114 In all models we set an weakly informative prior for the variance σ^2 , such that:

$$\sigma^2 \sim \text{halfCauchy}(0, 30000)\tag{9}$$

115 A summary of the priors used can be seen in Table 1. Bayesian inference was conducted using
116 RStan v2.7.0 [21, 22] running in R v3.2.1 [23].

117 **Part 2. Estimating total mortality using the catch curve**

118 The length-at-age dataset of *M. japonica* can be used as a representative sample of the number
119 of individuals within each age-class if we assume that sampling was opportunistic, and non-
120 selective across each age- or size-class. We also assume that there is limited migration in and out
121 of this population. With these assumptions, counting the number of individuals captured in each
122 age-class represents the population age structure, which can be used to construct a catch curve.

123 Catch curves are especially useful for data-poor species lacking stock assessments [24,25]. The
124 frequency of individuals in older or larger classes decreases due to a combination of natural and
125 fishing mortality. If fishing is non-selective with respect to size, the total mortality rate Z , which
126 is a combination of both fishing mortality F and natural mortality M , can be estimated using a
127 linear regression as the slope of the natural log of the number of individuals in each class [26].
128 This information is very valuable when inferring whether fishing mortality F is unsustainable.
129 We calculate Z as the slope of the regression of the catch curve, including only those ages or sizes
130 that are vulnerable to the fishery.

131 We removed age-classes that had zero individuals in our sample to be able to take the natural

132 logarithm of the count. Because there is uncertainty associated with the dataset (due to its rel-
133 atively small size), we resampled a subset of the dataset 20,000 times, after randomly removing
134 20% of the points. This allowed us to quantify uncertainty in our estimate of Z . For each subset,
135 we computed the age-class with the maximum number of samples, and removed all age-classes
136 younger than this peak. With the remaining age-classes, we fit a linear regression to estimate the
137 slope which is equivalent to $-Z$. This method for estimating mortality relies on two assumptions
138 of the selectivity of the fishery. First, catch is not size-selective once individuals are vulnerable
139 to the fishery. Second, if young age-classes are less abundant than older age-classes, they are
140 assumed to have lower catchability. This is why we removed the younger age-classes before the
141 “peak” abundance of each sample, as this will affect the steepness of the slope.

142 **Part 3. Estimating *M. japonica* maximum population growth rate**

143 Maximum intrinsic population growth rates r_{max} can be estimated based on a simplified version
144 of the Euler-Lotka equation [27, 28]. We use the following version of this equation to calculate
145 r_{max} . Unlike previous estimates of r_{max} for chondrichthyan species [12, 29, 30], this equation
146 accounts for juvenile mortality [31]:

$$l_{\alpha_{mat}} b = e^{r_m \alpha_{mat}} - e^{-M} (e^{r_m})^{\alpha_{mat}-1} \quad (10)$$

147 where $l_{\alpha_{mat}}$ is survival to maturity and is calculated as $l_{\alpha_{mat}} = (e^{-M})^{\alpha_{mat}}$, b is the annual
148 reproductive output of daughters, α_{mat} is age at maturity in years, and M is the instantaneous
149 natural mortality. We then solve equation 10 for r_{max} using the `nlm.imb` function in R. To ac-
150 count for uncertainty in input parameters, we use a Monte Carlo approach and draw values from
151 parameter distributions to obtain 10,000 estimates of r_{max} . Next we describe how we determined
152 each parameter distribution.

153 **Annual reproductive output (b)** Adult female mobulid rays only have one active ovary and
154 uterus where a single pup grows. This sets the upper bound of annual fecundity to one pup per
155 year [14], and assuming a 1:1 sex ratio, results in an estimate of b of 0.5 female pups per year. It is
156 possible female devil rays have a biennial cycle of reproduction where one pup is produced every
157 two years, as in manta rays [12], so the lower bound for our estimate of b is 0.25 female pups per
158 year. Thus we draw b from a uniform distribution bound between 0.25 and 0.5.

159 **Age at maturity (α_{mat})** There are no direct estimates of age at maturity for any mobulid ray,
160 but using age and growth data from Cuevas-Zimbrón (2013) [13] and a size at maturity of 200 cm
161 DW from Serrano-López (2009) [32], we assume *M. japonica* individuals reach sexual maturity
162 after 5-6 years. Thus we draw α_{mat} from a uniform distribution bound between 5 and 6.

163 **Natural mortality (M)** We estimate natural mortality as the reciprocal of average lifespan:
164 $M = 1/\omega$ where average lifespan ω is $(\alpha_{mat} + \alpha_{max})/2$. We used this estimate of M to cal-
165 culate survival to maturity $l_{\alpha_{mat}}$ as $(e^{-M})^{\alpha_{mat}}$. This method produces realistic estimates of r_{max}
166 when accounting for survival to maturity [31]. We also use our estimate of Z from Part 2, which
167 represents both natural and fishing mortality, to contextualize our estimate of M . More specif-
168 ically, our estimate of Z sets the upper bound for our estimate of M . We calculated maximum
169 age (α_{max}) based on the results of our analysis in Part 1. We therefore calculate M iteratively
170 by drawing values of α_{mat} (described in the section above) and α_{max} from uniform distributions
171 bound between the ranges mentioned.

172 **Part 4. Comparison of *Mobula* r_{max} among chondrichthyans**

173 We re-estimate r_{max} for the 94 chondrichthyans with complete life history data examined in
174 [12,30,31] using equation 10. We also update estimates of r_{max} for manta rays (*Manta* spp.) from
175 Dulvy et al. 2014 [12], as a comparison with a closely related species.

176 **Results**

177 **Part 1: Re-fitting the growth curve for *Mobula japonica***

178 The Bayesian model with strong priors yielded a lower estimate of k (0.12 year^{-1}) and a higher
179 estimate of L_{∞} (2995 cm DW) than the estimates based on weaker and uninformative priors
180 (Table 2, Fig. 1). The asymptotic size in the model with strong priors was closest to the maximum
181 observed size for this species (Fig. 2). Estimates of k were lowest in the model with strong priors
182 and highest in the model with uninformative priors (Table 2, Fig. 1).

183 **Part 2. Estimating total mortality using the catch curve**

184 Our catch curve analysis yielded a median estimate of $Z = 0.254 \text{ year}^{-1}$, with 95% of bootstrapped
185 estimates ranging between 0.210 and 0.384 year^{-1} (Fig. 3). There were no devil rays aged 12 or 13,
186 and therefore these age-classes were removed from the catch curve analysis before fitting each
187 regression. Because these age classes are some of the oldest, removing these points is likely to
188 provide more conservative estimates of total mortality. As a reference, we also ran the models
189 without removing these age-classes but adding one to the number of individuals in age-class
190 and got a very similar Z estimate ($\approx 0.23 \text{ year}^{-1}$). Assuming Z is approximately 0.25 year^{-1} is
191 therefore a relatively conservative estimate of total mortality; we infer natural mortality M of M .
192 *japonica* must be less than 0.25 year^{-1} or that 22.1% of the population was killed each year from a
193 combination of natural and fishing mortality.

194 **Part 3. Maximum population growth rate r_{max} of the Spinetail Devil Ray**

195 From Part 1, we estimated that maximum lifespan was between 15 and 20 years. Combining this
196 with estimated age at maturity, the median estimates of average lifespan for the Spinetail Devil
197 Ray was 11.5 years, and therefore the median natural mortality M estimate was 0.087 year^{-1} . From
198 Part 2, we found that mortality M had an upper bound of 0.25 year^{-1} (assuming $Z = M$). Using

199 this information to create a bounded distribution for natural mortality in equation 10, we found
200 the median maximum intrinsic rate of population increase r_{max} for devil rays is 0.077 year⁻¹ (95th
201 percentile = 0.042–0.108).

202 **Part 4. Comparing *Mobula* r_{max} to other chondrichthyans**

203 Devil and manta rays have low intrinsic rate of population increase relative to other chondrichthyan
204 species (Fig. 4). Among species with similar somatic growth rates, the Spinetail Devil Ray has
205 the lowest r_{max} value (black diamond in Fig. 4a). This contrast is strongest when excluding deep-
206 water chondrichthyans (white circles in Fig. 4), which tend to have much lower rates of population
207 increase than shallow-water ones [33]. Our estimation of r_{max} for manta rays (grey diamond in
208 Fig. 4) are comparable with our estimates for the Spinetail Devil Ray, albeit slightly lower (me-
209 dian of 0.068 year⁻¹, 95th percentile = 0.045–0.088). Values of r_{max} for other large planktivorous
210 elasmobranchs (Whale and Basking Sharks) are relatively high compared to manta and devil rays.

211 **Discussion**

212 In this study, we examined multiple lines of evidence that suggest devil rays have relatively low
213 productivity, and hence high risk of extinction compared to other chondrichthyans. The r_{max} of
214 the Spinetail Devil Ray is comparable to that of manta rays, and much lower than that of other
215 large planktivorous shallow-water chondrichthyans such as the Whale Shark and the Basking
216 Shark (Fig. 4). We conclude the comparable extinction risks of devil and manta rays, coupled with
217 the ongoing demand for their gill plates, suggest that conferring a similar degree of protection to
218 all mobulids is warranted.

219 Next we consider three key questions that arise from our analyses: (1) Why do mobulid rays
220 have such low productivity? (2) Can growth estimates be improved with prior knowledge? (3)
221 Can small-scale fisheries cause local declines in devil ray populations?

222 **Why do mobulid rays have such low productivity?**

223 We found that the Spinetail Devil Ray has similar productivity to manta rays, despite this species
224 being half the size of the manta rays. This result suggests that smaller devil ray species are also
225 likely to have very low productivity, probably due to their very low reproductive rates. Mobulid
226 rays have at most a single pup annually or even biennially, while the Whale Shark can have litter
227 sizes of up to 300 pups [34], therefore increasing the potential ability of this species to replenish
228 its populations (notwithstanding differences in juvenile mortality). The Basking Shark has a litter
229 size of six pups, which partly explains why its r_{max} is intermediate between mobulids and the
230 Whale Shark. While mobulids mature relatively later with respect to their total lifespan than
231 Basking Sharks and relatively earlier than Whale Sharks, they have lower lifetime fecundity than
232 both Whale and Basking Sharks, limiting their productivity.

233 Our results are consistent with the correlation between low somatic growth rates, later matu-
234 ration, large sizes, and elevated extinction risk that has been found in other marine fishes [35, 36]
235 (Fig. 4a). For example, in tunas and their relatives, somatic growth rate is the best predictor of
236 overfishing, such that species with slower growth are more likely to be overfished as fishing mor-
237 tality increases than species with faster growth [37], likely because the species that grow faster
238 mature earlier.

239 **Can growth estimates be improved with prior knowledge?**

240 Our method for estimating growth rate for the Spinetail Devil Ray provided lower estimates of
241 the growth coefficient k than was reported in the original study [13], especially when we used
242 strongly informative priors. When using strong priors the estimated asymptotic size was very
243 close to the expectation of it being 90% of maximum size. On the other hand, our scenario with
244 uninformative priors provided growth coefficient k estimates that are very similar to the original
245 estimates, which were obtained by nonlinear least squares minimization (Fig. 2b). Our growth
246 estimates from the model with strong priors are consistent with our expected values of k if length-

247 at-age data were available for larger individuals. Given that the length-at-age data available only
248 includes individuals up to two-thirds of the maximum size recorded for *M. japonica*, we believe
249 that our approach provides more plausible estimates of growth rates when data are sparse. Our
250 approach provides further evidence that Bayesian estimation is useful for data-sparse species as
251 the available life history information can be easily incorporated in the form of prior distributions,
252 particularly when missing samples of the largest or smallest individuals [15]. Incorporating prior
253 information when fitting growth curves is an alternative to fixing model parameters, which often
254 biases growth estimates [38]. In other words, using Bayesian inference allows us to incorpo-
255 rate out-of-sample knowledge of observed maximum sizes and sizes at birth, thus improving our
256 estimates of growth rates and asymptotic size [15].

257 **Can small-scale fisheries cause local declines in devil ray populations?**

258 The estimate of fishing mortality we calculated from the catch curve ($Z - M = F = 0.163$
259 year^{-1}) is twice as high than our estimate of r_{max} , which also represents the fishing mortality F
260 expected to drive this species to extinction ($F_{ext} = 0.077 \text{ year}^{-1}$) [28]. Even though our estimate of
261 fishing mortality is highly uncertain (Fig. 3b), the large discrepancy between our estimates of F
262 and F_{ext} suggests that even if we are overestimating fishing mortality it was likely greater than
263 F_{ext} . Hence we infer that before the fishery ceased in 2007, the Spinetail Devil Ray population
264 we examined was probably being fished unsustainably at a rate high enough to lead to eventual
265 local extinction. Many teleost fisheries support fishing mortalities that are many times larger
266 than natural mortality because of strong density dependence. However, mobulids likely have
267 low capacity to compensate for fishing, because their large offspring and low fecundity suggest
268 weak density-dependent regulation of populations [39, 40].

269 The major caveats of using a catch curve analysis to estimate total mortality are that it as-
270 sumes there is no size selectivity in catch, recruitment is constant, the population is closed, and
271 that the catch is a large enough sample to sufficiently represent population age structure. These

272 assumptions are also required in age and growth studies when using length-at-age data. Thus,
273 our approach of estimating fishing mortality could be applied to other chondrichthyan growth
274 studies, assuming that fishing is not systematically size selective and that metapopulation dy-
275 namics are not influencing the sample. Whether or not this latter assumption is valid for highly
276 migratory elasmobranch species has yet to be tested.

277 Unregulated small-scale artisanal fisheries are targeting mobulids throughout the world [4,
278 5]. Our findings imply that there is little room for unmanaged artisanal fisheries to support
279 sustainable international exports of gill plates or even domestic meat markets. Furthermore, the
280 unsustainable fishing mortality stemming from the removal of relatively few individuals by an
281 artisanal fishery suggests we urgently need to understand the consequences of bycatch of mobulid
282 rays in industrial trawl, long line and purse seine fisheries [4, 8]. The combination of high catch
283 rates and low post-release survival suggest fishing mortality rates need to be understood and
284 potentially minimized to ensure the future persistence of these species.

285 **Acknowledgements**

286 We thank the fisherman of the fishing camp “Punta Arenas de la Ventana”, Baja California Sur,
287 Mexico, for allowing collection of specimens and biological material. Field and lab work was
288 supported by F. Galvan, N. Serrano, I. Mendez, A. Medellín, L. Castillo and C. Rodríguez, E. Díáz,
289 J. M. Alfaro and E. Bravo. We thank S. C. Anderson for statistical advice.

290 The original fieldwork was supported by the project “Historia Natural, Movimientos, Pes-
291 quería y Criaderos, Administración de Mantas Mobulidas en el Golfo de California” of the Mon-
292 terey Bay Aquarium. This research was funded by the J. Abbott /M. Fretwell Graduate Fellowship
293 in Fisheries Biology (SAP), NSERC Discovery and Accelerator Grants (NKD), a Canada Research
294 Chair (NKD), an NSF Postdoctoral Fellowship in Math and Biology (HKK; DBI-1305929), and
295 grants to NKD from the John D. and Catherine T. MacArthur Foundation, the Leonardo DiCaprio
296 Foundation, Disney Conservation Fund, and the Wildlife Conservation Society.

297 **Supporting Information**

298 **References**

- 299 1. O'Malley MP, Lee-Brooks K, Medd HB. The Global Economic Impact of Manta Ray Watch-
300 ing Tourism. PLoS ONE. 2013 may;8(5):e65051. Available from: <http://dx.doi.org/10.1371/journal.pone.0065051>.
301
- 302 2. Mundy-Taylor V, Crook V. Into the deep: Implementing CITES measures for commercially-
303 valuable sharks and manta rays. Cambridge: TRAFFIC; 2013.
- 304 3. Zeeberg J, Corten A, de Graaf E. Bycatch and release of pelagic megafauna in in-
305 dustrial trawler fisheries off Northwest Africa. Fisheries Research. 2006 may;78(2-
306 3):186–195. Available from: <http://www.sciencedirect.com/science/article/pii/S0165783606000403>.
307
- 308 4. Croll DA, Dewar H, Dulvy NK, Fernando D, Francis MP, Galván-Magaña F, et al. Vul-
309 nerabilities and fisheries impacts: the uncertain future of manta and devil rays. Aquatic
310 Conservation: Marine and Freshwater Ecosystems. 2015 jan;p. n/a–n/a. Available from:
311 <http://dx.doi.org/10.1002/aqc.2591>.
- 312 5. Couturier LIE, Marshall AD, Jaine FRA, Kashiwagi T, Pierce SJ, Townsend KA, et al. Biology,
313 ecology and conservation of the Mobulidae. Journal of Fish Biology. 2012;80(5):1075–1119.
314 Available from: <http://dx.doi.org/10.1111/j.1095-8649.2012.03264.x>.
- 315 6. Poder Ejecutivo Federal. NOM-029-PESC-2006, Responsible Fisheries of Sharks and Rays,
316 Specifications for their Use (in Spanish). Ciudad de México; 2007.
- 317 7. Heinrichs S, O'Malley M, Medd H, Hilton P. Manta Ray of Hope 2011 Report: The Global
318 Threat to Manta and Mobula Rays. San Francisco, CA: WildAid; 2011.

- 319 8. Francis MP, Jones EG. Movement, depth distribution and survival of spinetail devilrays
320 (*Mobula japonica*) tagged and released from purse-seine catches in New Zealand. Aquatic
321 Conservation: Marine and Freshwater Ecosystems. in press;
- 322 9. Musick JA. Criteria to Define Extinction Risk in Marine Fishes: The American Fisheries
323 Society Initiative. Fisheries. 1999 dec;24(12):6–14. Available from: [http://dx.doi.org/
324 10.1577/1548-8446\(1999\)024<0006:CTDERI>2.0.CO2](http://dx.doi.org/10.1577/1548-8446(1999)024<0006:CTDERI>2.0.CO2).
- 325 10. Reynolds JD, Dulvy NK, Goodwin NB, Hutchings Ja. Biology of extinction risk
326 in marine fishes. Proceedings of the Royal Society B. 2005 nov;272(1579):2337–44.
327 Available from: [http://www.pubmedcentral.nih.gov/articlerender.fcgi?artid=
328 1559959&tool=pmcentrez&rendertype=abstract](http://www.pubmedcentral.nih.gov/articlerender.fcgi?artid=1559959&tool=pmcentrez&rendertype=abstract).
- 329 11. Jennings S, Reynolds JD, Mills SC. Life history correlates of responses to fisheries exploita-
330 tion. Proceedings of the Royal Society B. 1998;265:333–339.
- 331 12. Dulvy NK, Pardo SA, Simpfendorfer CA, Carlson JK. Diagnosing the dangerous demog-
332 raphy of manta rays using life history theory. PeerJ. 2014 may;2:e400. Available from:
333 <https://peerj.com/articles/400>.
- 334 13. Cuevas-Zimbrón E, Sosa-Nishizaki O, Pérez-Jiménez J, O’Sullivan J. An analysis of the fea-
335 sibility of using caudal vertebrae for ageing the spinetail devilray, *Mobula japonica* (Müller
336 and Henle, 1841). Environmental Biology of Fishes. 2013;96(8):907–914. Available from:
337 <http://dx.doi.org/10.1007/s10641-012-0086-2>.
- 338 14. Notarbartolo-Di-Sciara G. A revisionary study of the genus *Mobula* Rafinesque, 1810
339 (Chondrichthyes: Mobulidae) with the description of a new species. Zoological Journal of
340 the Linnean Society. 1987 sep;91(1):1–91. Available from: [http://dx.doi.org/10.1111/
341 j.1096-3642.1987.tb01723.x](http://dx.doi.org/10.1111/j.1096-3642.1987.tb01723.x).

- 342 15. Siegfried K, Sansó B. Two Bayesian methods for estimating parameters of the von Berta-
343 lanffy growth equation. *Environmental Biology of Fishes*. 2006;77(3-4):301–308. Available
344 from: <http://dx.doi.org/10.1007/s10641-006-9112-6>.
- 345 16. White WT, Giles J, Potter IC. Data on the bycatch fishery and reproductive biol-
346 ogy of mobulid rays (Myliobatiformes) in Indonesia. *Fisheries Research*. 2006 dec;82(1-
347 3):65–73. Available from: [http://www.sciencedirect.com/science/article/pii/
348 S0165783606002992](http://www.sciencedirect.com/science/article/pii/S0165783606002992).
- 349 17. White WT, Last PR, Stevens JD, Yearsley GK, Fahmi, Dharmadi. Economically important
350 sharks and rays of Indonesia. Canberra: Australian Centre for International Agricultural
351 Research; 2006. Available from: <http://aciarc.gov.au/publication/mn124>.
- 352 18. Paulin CD, Habib G, Carey CL, Swanson PM, Voss GJ. New records of *Mobula japonica* and
353 *Masturus lanceolatus*, and further records of *Luvaris imperialis* (Pisces: Mobulidae, Molidae,
354 Louvaridae) from New Zealand. *New Zealand Journal of Marine and Freshwater Research*.
355 1982 mar;16(1):11–17. Available from: [http://dx.doi.org/10.1080/00288330.1982.
356 9515943](http://dx.doi.org/10.1080/00288330.1982.9515943).
- 357 19. Poortvliet M, Olsen JL, Croll DA, Bernardi G, Newton K, Kollias S, et al. A dated molec-
358 ular phylogeny of manta and devil rays (Mobulidae) based on mitogenome and nuclear
359 sequences. *Molecular phylogenetics and evolution*. 2015 feb;83:72–85. Available from:
360 <http://www.sciencedirect.com/science/article/pii/S1055790314003637>.
- 361 20. Froese R, Binohlan C. Empirical relationships to estimate asymptotic length, length at
362 first maturity and length at maximum yield per recruit in fishes, with a simple method to
363 evaluate length frequency data. *Journal of Fish Biology*. 2000 apr;56(4):758–773. Available
364 from: <http://doi.wiley.com/10.1006/jfbi.1999.1194>.
- 365 21. Stan Development Team. Stan Modeling Language User’s Guide and Reference Manual,
366 Version 2.7.0; 2015. Available from: <http://mc-stan.org/>.

- 367 22. Stan Development Team. Stan: A C++ Library for Probability and Sampling, Version 2.7.0;
368 2015. Available from: <http://mc-stan.org/>.
- 369 23. R Core Team. R: A Language and Environment for Statistical Computing. Vienna, Austria;
370 2015. Available from: <https://www.r-project.org/>.
- 371 24. Thorson JT, Prager MH. Better Catch Curves: Incorporating Age-Specific Natural Mor-
372 tality and Logistic Selectivity. *Transactions of the American Fisheries Society*. 2011
373 mar;140(2):356–366. Available from: [http://tandfprod.literatumonline.com/doi/](http://tandfprod.literatumonline.com/doi/abs/10.1080/00028487.2011.557016)
374 [abs/10.1080/00028487.2011.557016](http://tandfprod.literatumonline.com/doi/abs/10.1080/00028487.2011.557016).
- 375 25. Hordyk A, Ono K, Valencia S, Loneragan N, Prince J. A novel length-based empirical
376 estimation method of spawning potential ratio (SPR), and tests of its performance, for
377 small-scale, data-poor fisheries. *ICES Journal of Marine Science: Journal du Conseil*. 2015
378 jan;72(1):217–231. Available from: [http://icesjms.oxfordjournals.org/content/72/](http://icesjms.oxfordjournals.org/content/72/1/217.abstract)
379 [1/217.abstract](http://icesjms.oxfordjournals.org/content/72/1/217.abstract).
- 380 26. Ricker W. Computation and interpretation of biological statistics of fish populations. Ot-
381 tawa: Department of the Environment Fisheries and Marine Service; 1975.
- 382 27. Charnov EL, Schaffer WM. Life-History Consequences of Natural Selection: Cole’s Result
383 Revisited. *The American Naturalist*. 1973;107(958):791–793. Available from: [http://www.](http://www.jstor.org/stable/2459713)
384 [jstor.org/stable/2459713](http://www.jstor.org/stable/2459713).
- 385 28. Myers RA, Mertz G. The limits of exploitation: A precautionary approach. *Ecological*
386 *Applications*. 1998;8(1):165–169.
- 387 29. Hutchings JA, Myers RA, García VB, Lucifora LO, Kuparinen A. Life-history correlates of
388 extinction risk and recovery potential. *Ecological Applications*. 2012 jan;22(4):1061–1067.
389 Available from: <http://dx.doi.org/10.1890/11-1313.1>.

- 390 30. García VB, Lucifora LO, Myers RA. The importance of habitat and life history to extinc-
391 tion risk in sharks, skates, rays and chimaeras. *Proceedings of the Royal Society B*. 2008
392 jan;275:83–89. Available from: [http://www.pubmedcentral.nih.gov/articlerender.](http://www.pubmedcentral.nih.gov/articlerender.fcgi?artid=2562409&tool=pmcentrez&rendertype=abstract)
393 [fcgi?artid=2562409&tool=pmcentrez&rendertype=abstract](http://www.pubmedcentral.nih.gov/articlerender.fcgi?artid=2562409&tool=pmcentrez&rendertype=abstract).
- 394 31. Pardo SA, Kindsvater HK, Reynolds JD, Dulvy NK. Maximum intrinsic rate of population
395 increase in sharks, rays, and chimaeras: the importance of survival to maturity. *Canadian*
396 *Journal of Fisheries and Aquatic Sciences*. in review;
- 397 32. Serrano-López J. Estudio comparativo de la reproducción de tres especies del género *Mob-*
398 *ula* (Chondrichthyes: Mobulidae) en el suroeste del Golfo de California, México [MSc The-
399 sis]. BCS, La Paz; 2009.
- 400 33. Simpfendorfer CA, Kyne PM. Limited potential to recover from overfishing raises concerns
401 for deep-sea sharks, rays and chimaeras. *Environmental Conservation*. 2009 nov;36(02):97.
402 Available from: http://www.journals.cambridge.org/abstract_S0376892909990191.
- 403 34. Joung SJ, Chen CT, Clark E, Uchida S, Huang WYP. The whale shark, *Rhincodon typus*, is a
404 livebearer: 300 embryos found in one 'megamamma' supreme. *Environmental Biology of*
405 *Fishes*. 1996;46:219–223.
- 406 35. Jennings S, Dulvy NK. Beverton and Holt's Insights into Life History Theory: Influence,
407 Application and Future Use. In: Payne AI, Cotter AJR, Potter ECE, editors. *Advances in*
408 *Fisheries Science*. Oxford: Blackwell Publishing Ltd.; 2008. p. 434–450. Available from:
409 <http://dx.doi.org/10.1002/9781444302653.ch18>.
- 410 36. Dulvy NK, Sadovy Y, Reynolds JD. Extinction vulnerability in marine populations. *Fish*
411 *and Fisheries*. 2003;4:25–64.
- 412 37. Juan-Jordá MJ, Mosqueira I, Freire J, Dulvy NK. Life history correlates of marine fisheries
413 vulnerability: a review and a test with tunas and mackerel species. In: Briand F, editor.

- 414 Marine extinctions - patterns and processes. CIESM Workshop Monograph n°45. Monaco:
415 CIESM Publisher; 2013. p. 113–128.
- 416 38. Pardo SA, Cooper AB, Dulvy NK. Avoiding fishy growth curves. *Methods in Ecology*
417 *and Evolution*. 2013 apr;4(4):353–360. Available from: [http://dx.doi.org/10.1111/](http://dx.doi.org/10.1111/2041-210x.12020)
418 [2041-210x.12020](http://dx.doi.org/10.1111/2041-210x.12020).
- 419 39. Forrest RE, Walters CJ. Estimating thresholds to optimal harvest rate for long-lived, low-
420 fecundity sharks accounting for selectivity and density dependence in recruitment. *Cana-*
421 *dian Journal of Fisheries and Aquatic Sciences*. 2009;66:2062–2080.
- 422 40. Kindsvater HK, Mangel M, Reynolds JD, Dulvy NK. Ten principles from evolutionary ecol-
423 ogy essential for effective marine conservation. *Ecology and Evolution*. 2016;Available
424 from: <http://doi.org/10.1002/ece3.2012>.

Table 1: Priors used in the three different Bayesian von Bertalanffy growth models.

Model	Prior for k	Prior for L_∞	Prior for L_0	Prior for $kappa$	Prior for σ^2
Strong	$Beta(1.05, 1.5)$	$Normal(3100 * kappa, 100)$	$Normal(880, 200)$	$Gamma(1000, 990)$	$halfCauchy(0, 30000)$
Weaker	$Beta(1.05, 1.1)$	$Normal(3100 * kappa, 400)$	$Normal(880, 300)$	$Gamma(200, 198)$	$halfCauchy(0, 30000)$
Uninformative	$Uniform(0, 2)$	$Uniform(0, 4000)$	$Uniform(0, 2000)$	$Uniform(0.7, 1.3)$	$halfCauchy(0, 30000)$

Table 2: Mean von Bertalanffy growth parameter estimates for the three Bayesian models with differing priors. Values inside square brackets are the 95% credible intervals (CI).

Model	Estimate of L_∞	Estimate of k	Estimate of σ^2
Strong priors	2999 mm [2711-3295]	0.12 year ⁻¹ [0.086-0.169]	0.106 [0.088-0.13]
Weaker priors	2515 mm [2232-3018]	0.221 year ⁻¹ [0.11-0.353]	0.102 [0.084-0.124]
Uninformative priors	2386 mm [2175-2744]	0.268 year ⁻¹ [0.144-0.406]	0.102 [0.084-0.124]

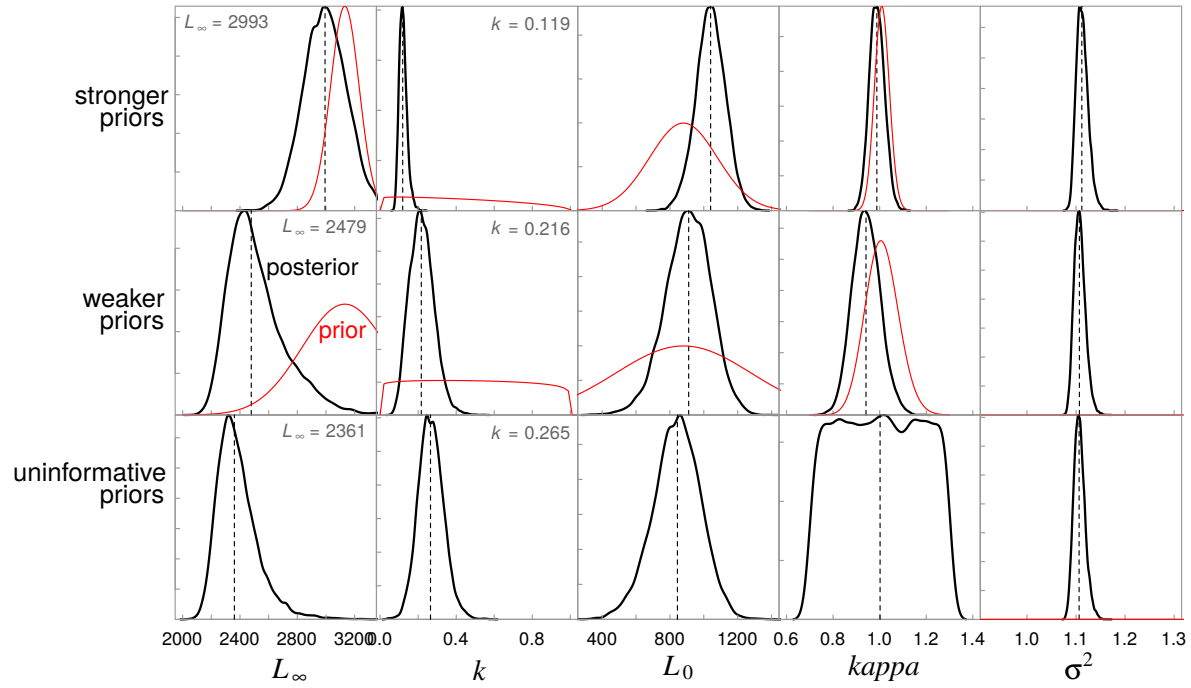


Figure 1: Prior and posterior distributions for the Spinetail devil Ray (*Mobula japonica*) von Bertalanffy growth parameters (L_∞ , k , and L_0) and the error term (σ^2) for the three Bayesian models with strong, weaker, and uninformative priors. Median values are shown by the dashed lines, posterior distributions by the black lines, and prior distributions by the red lines. No prior distributions are shown when priors are uninformative (uniform distribution).

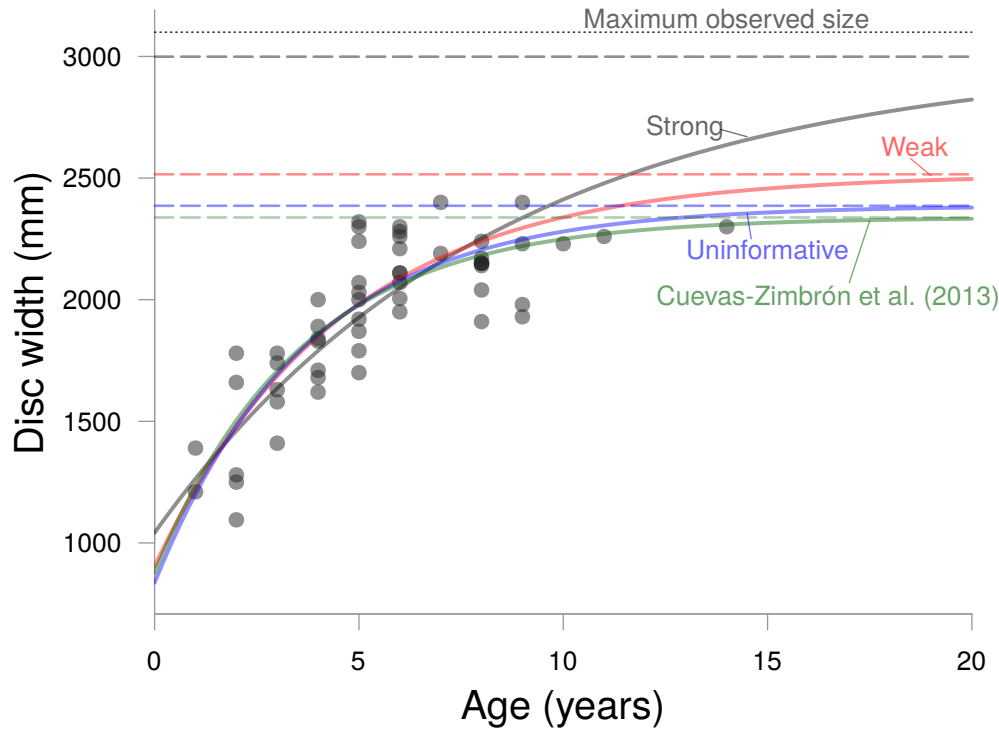


Figure 2: Length-at-age data for the Spinetail Devil Ray *Mobula japonica* showing the Bayesian von Bertalanffy growth curve fits for models with strong (grey), weaker (red), and uninformative (blue) priors, as well as the original model fit from Cuevas-Zimbrón et al. (2013). Dashed lines show the asymptotic size (L_{∞}) estimates for each model. Dotted line represents the maximum known size for the species.

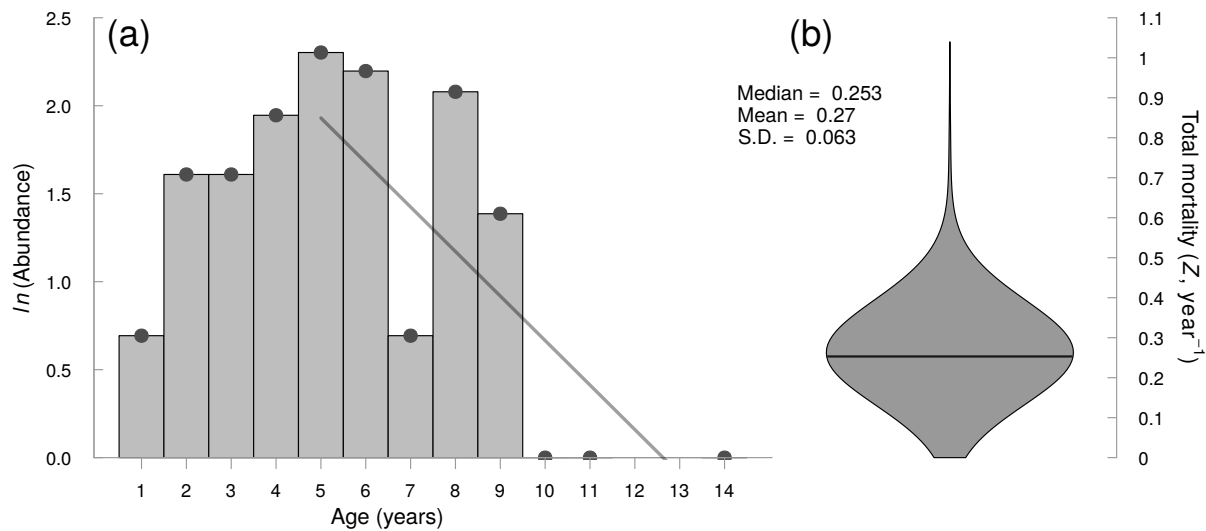


Figure 3: Estimation of total mortality Z from bootstrapped catch composition data for the Spine-tail Devil Ray (*Mobula japonica*) from Cuevas-Zimbrón et al. (2013). (a) Catch curve of natural log abundance at age. The regression lines represent the estimated slopes when omitting different age-class subsets (as shown by the horizontal extent of each line), and resampling 80% of the data. Note that individual estimates of Z differ in the number of age-classes included for its computation, resulting in regression lines of different lengths. (b) Violin plot of estimated total mortality (Z) values calculated using the bootstrap resampling method. Estimates from different age-classes suggest an estimate of $Z \approx 0.25 \text{ year}^{-1}$. The median is shown by the dark grey line.

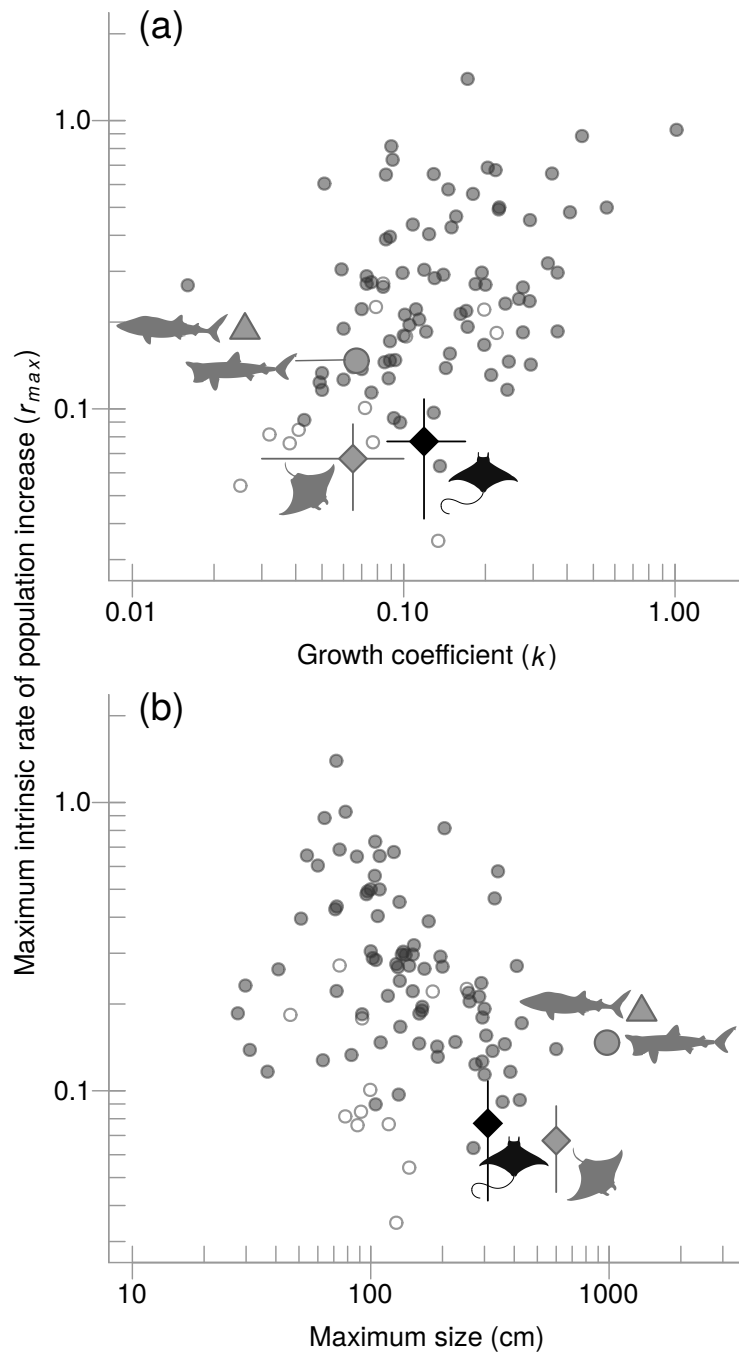


Figure 4: Comparison of maximum intrinsic rate of population increase (r_{max}) for 96 elasmobranch species arranged by (a) growth coefficient k and (b) maximum size. Small open circles represent deep sea species while small grey circles denote oceanic and shelf species. Four species are highlighted using silhouettes and larger symbols: the Spinetail Devil Ray (*Mobula japonica*) is shown by the black diamond, while the manta ray (*Manta spp.*), Whale Shark (*Rhincodon typus*) and Basking Shark (*Cetorhinus maximus*) are represented by the grey diamond, triangle and circle, respectively.